Preparation and properties of hydroxyapatite filters for microbial filtration

Lei Yang, Xiaoshan Ning *, Kexin Chen, Heping Zhou

*State Key Laboratory of New Ceramics and Fine Processing, Department of Materials Science and Engineering,
Tsinghua University, Beijing 100084, China*

Abstract

Preparation and properties of two kinds of hydroxyapatite filters, filter cloths and porous ceramics, were investigated. The filter cloth was prepared by depositing nanosize ceramic hydroxyapatite on a cotton fabric. The porous ceramic with pore size of several micrometers or less was fabricated by using water soluble starch as a pore former, and its permeability was controlled by adding insoluble starch. Bacterial filtration tests showed that the six-layer filter cloth can clear bacteria effectively, and the porous ceramic can remove 100% of the bacteria. Both the filter cloth and the porous ceramic can be used to clear or separate microbes.

1. Introduction

Many fatal infectious diseases, such as tuberculosis, acute lower respiratory infections and severe acute respiratory syndrome, are caused by bacteria or viruses. Since the spread of these causative microorganisms is mainly via airborne particles (mainly dusts) and water [1], it is of practical importance to develop filter materials for gaseous and aqueous treatment. The filtration materials are best to be nontoxic, especially for purification of domestically and medically used air or water. Moreover, in the sector of purification of microbe contaminated body fluids (blood, lymph, etc.), the optimal filtration materials should have enough biocompatibility with human cells as well. Hydroxyapatite (HA) is a very promising candidate because of its excellent biocompatibility and nontoxic hypostasis with organic tissues [2,3], and its adsorbability of bacteria and replication competent human virus [4,5].

On the other hand, the small size of microbes, which are usually 0.5–5 μm in diameter for bacteria and 10–500 nm for viruses, requires filters with fine structures and small pore sizes.

However, the current techniques for fabricating porous HA, such as starch consolidation and gelcasting of foams, allow formation of macropores (∼100 μm) but not of such small pores [6,7].

In the present work, two kinds of HA filters, a kind of flexible filter cloth and a kind of porous HA ceramic including a large amount of submicron pores were produced. The microstructures of the filters, the distribution of the pore size and the permeability of the porous ceramics were investigated. Finally, the microbial filtration property and removing efficacy of the filters were studied.

2. Experimental

2.1. Preparation of HA

HA was synthesized through a sol–gel method. Analytical pure $Ca(NO_3)_2$ and $(NH_4)_2HPO_4$ were dissolved into ion-free water separately and some $NH_3 \cdot H_2O$ was also added. The solutions were then mixed together to form a sol at room temperature which was kept at pH 8 for 24 h to change into gel. The gel was dried at 80 °C for another 24 h and then calcined at 550 °C for 5 h to produce HA powders. The powders were ground and sieved through 100, 200 and 400 mesh sieves, respectively. The scanning electron microscope (SEM) image

* Corresponding author. Tel.: +86 10 6277 2548; fax: +86 10 6277 2548.
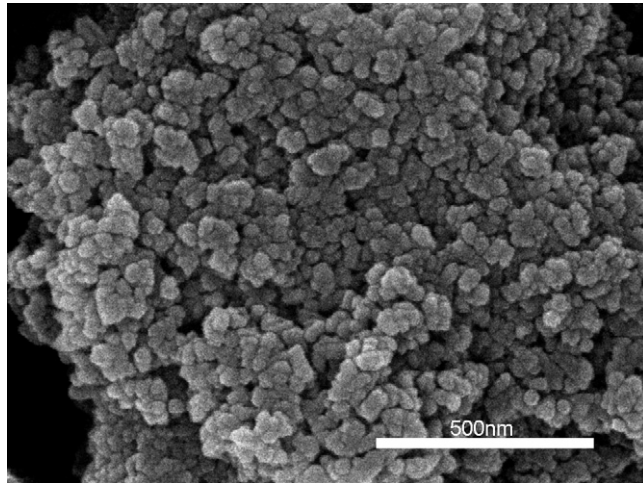*E-mail address:* caike@tsinghua.edu.cn (X. Ning).

Fig. 1. SEM image of nanosize HA powder prepared by a sol–gel method.

revealed that the HA particle was composed of about 20–100 nm nanosize grains, as shown in Fig. 1.

2.2. Preparation of filter cloth

Cotton fabric with threads per centimeter of 25×23 was used for preparing the filter cloth. As there is no standard method to characterize the pore or void size on the woven or knitted fabric, the pore size was measured from SEM images of the fabric as shown in Fig. 2. The quasi-square pores created by the crossing threads are in the length of 100–200 μm, and the distance between neighboring two filaments in a thread is less than tens microns.

The first step to prepare the filter cloth was to mix the HA powder with ion-free water to produce a slurry of 20 wt% solids. Fabrics of $5 \text{ cm} \times 5 \text{ cm}$ in size were dipped into the slurry for 6 h and the slurry was stirred to prevent uneven sediment of HA powder. The HA deposited fabrics were then dried at 50 °C and sewed into different layers.
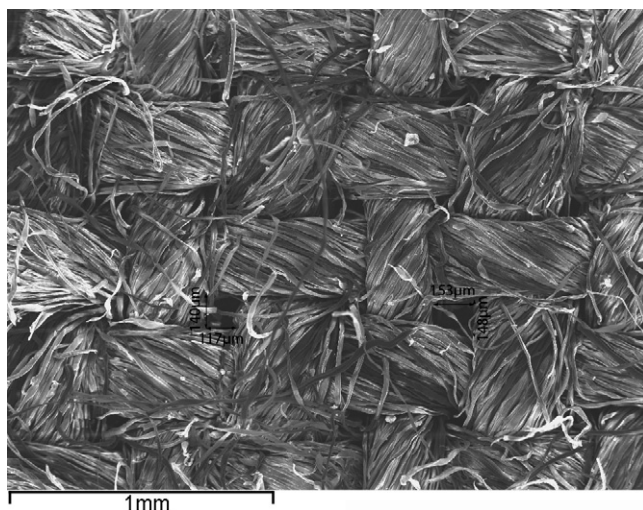

Fig. 2. SEM image of the cotton fabric. The quasi-square pores created by the crossing threads are in the length of 100–200 μm.

Table 1
Volume fractions of starch added in different samples

Sample	I	W1	W2	W3	M1	M2	M3	M4
WS (%)	–	30	60	80	15	15	15	30
IS (%)	30	–	–	–	15	30	45	30
HA (%)	70	70	40	20	70	55	40	40

2.3. Preparation of porous ceramic

Water soluble starch (WS, Chengdu Hongbo Co., China, water solubility ≥96%) was dissolved in ion-free water and then mixed with HA powder in a planetary mill for 12 h. The slurry was dried at 60 °C for 12 h to obtain starch-coated HA powders. In order to obtain interconnected pores, commercial insoluble starch (IS, Sichuan LeJun Co., China) with average granule size of 43 μm was added in the slurry in some cases. Table 1 shows the volume fractions of starch added in different samples.

Green ceramic bodies, 20 mm in diameter and 4 mm thick, were formed by pressing the powder uniaxially at 4 MPa for 2 min. They were heated up to 550 °C at a heating rate of 0.5 °C/min to burn out the starch, and finally sintered at 1200 °C with a dwell time of 3 h.

2.4. Characterization

The microstructures of the filter cloth and the porous ceramic were characterized by SEM (HITACHI S-450 and JSM-6460LV). Samples were gold-coated and observed at an accelerating voltage of 10–20 kV.

Phase identification of the synthesized HA and the sintered ceramic was carried out by X-ray diffraction (XRD). XRD patterns were collected by using a RIKAGU D/Max-RB diffractometer with Cu Kα radiation (40 kV, 120 mA).

2.5. Porosity of porous ceramics

The total porosity of the ceramic was calculated as

$$P_{\text{total}} = \frac{\rho_{\text{th}} - \rho_{\text{m}}}{\rho_{\text{th}}} \tag{1}$$

where ρ_{th} is the theoretical density of HA (3.12 g/cm^3), and ρ_{m} is the measured density of the porous ceramic.

The porosity of the open pores was measured according to the Chinese government standard GB/T 1966–1996 [8]. A porous ceramic of weight m_1 was immersed in a container filled with distilled water. The container was placed in vacuum to force the water into the pores until no air bubble emerged from the ceramic. The weights of this saturated ceramic before and after it was removed form distilled water were recorded as m_3 and m_2, respectively. The open porosity, P_{open}, was then

$$P_{\text{open}} = \frac{m_2 - m_1}{m_2 - m_3} \tag{2}$$

2.6. Permeability of porous ceramics

Permeability is another important property of porous ceramics. However, there is no agreement on a single test and the fluid (liquid or gas) to be used. In the work, the permeability μ (m^2) of the porous ceramic was measured with pure nitrogen and calculated according to Darcy's law [9] and ISO 8841–1991 [10]:

$$\mu = 2.16 \times 10^{-6} \eta \times \frac{d}{D^2} \times \frac{q}{p_i - p_0} \times \frac{2 p_i}{p_i + p_0} \quad (3)$$

where η is the dynamic viscosity of nitrogen at the testing temperature, d and D the thickness and the diameter of the sample, respectively, q the volume flow of nitrogen gas passed through the sample, and p_i and p_0 are the constant pressures at the entrance and exit of the sample.

2.7. Microbial filtration test

Microbial filtration properties of two kinds of filters were tested by filtering *Escherichia coli* suspension, and the filtrate was assayed by the viable cell counting method. During each test, 5 ml phosphate buffered saline (PBS) diluted *E. coli* suspension containing about 10^5 cells/ml was filtrated through the filter cloth or porous ceramic, and then the filtrate (0.1 ml) was inoculated in the 20 ml LB agar plate with aerobic incubation at 37 °C for 24 h. The resultant colonies were counted and the removing percentage relative to controls without filtration was calculated. Three parallel plates were used for counting the viable cells and the counting was done in triplicate each time. The cross-section of the porous ceramic was observed by SEM (HITACHI S-450) after filtration.

3. Results and discussion

3.1. Filter cloth

The XRD pattern shown in Fig. 3a reveals that the particles deposited on the cotton fabric are composed of crystalline HA.
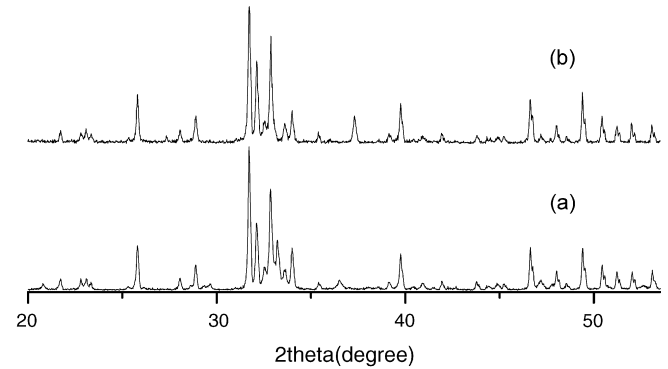

Fig. 3. XRD patterns of (a) synthesized HA powder and (b) porous ceramic sintered at 1200 °C.

The adhesion state of the particles deposited on the cloth was evaluated by SEM. Preliminary results indicate that HA powders passed through the 100 mesh sieve, with particle size as large as 140 μm, are too large to adhere, as the particles deposited on fabric are observed highly non-uniform and unstable, and the large particles can easily break away by strongly shaking the filter cloth.

Sieving the HA powder down to <40 μm results in a more uniform and adhered coating on fabric. The SEM image shown in Fig. 4a illustrates the morphology of the optimally coated fabrics. A relatively homogeneous HA layer of uniform thickness is formed on the filaments of the cloth, and some of the HA particles penetrate into the voids of the filaments. The filter cloth was further tested by strongly shaking and folding for several times, and no peeling-off of the particles occurred this time, which indicates that the HA particles well adhered to the fabric surface. This result can be confirmed by SEM observation, as shown in Fig. 4b, which reveals that HA particles still fill up the voids between neighboring filaments firmly after the shaking test. Although the adhesion strength between the HA particles and cotton fabric was not quantitatively determined in the work, it is reasonable to assume that the strong interaction is due to a mechanical
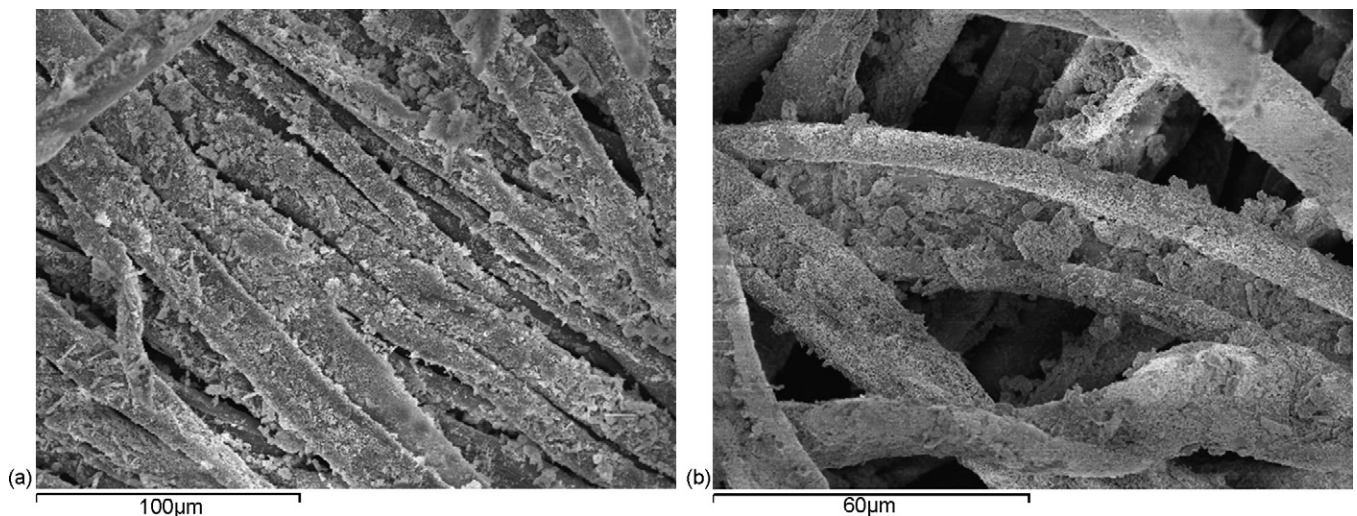

Fig. 4. SEM images of showing the (a) coating morphology for the optimally coated fabric and (b) well adhered HA particles filling the voids of filaments after the shaking test.
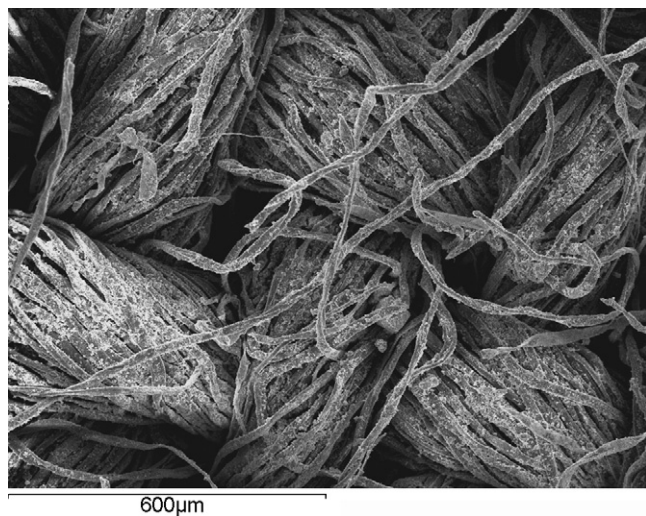
Fig. 5. The morphology of the quasi-square pores among crossing threads and voids among filaments after the HA was deposited.
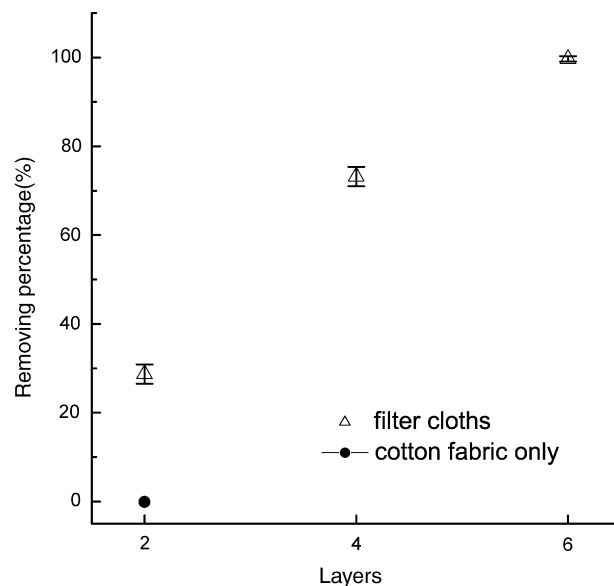

Fig. 6. Removing percentage of *E. coli* following filtration through filter cloths of different layers.

interlocking mechanism between the particles and the fabric. This result demonstrates the suitability of the filter cloth as a material for producing face masks or other respirators.

Although the HA particles adhered on the fabric can fill up some of the voids among the filaments, the filter cloth is still readily permeable as the previous pores or voids of the woven fabric are still predominant. Figs. 5 and 4b show that the previous quasi-square pores and most of the voids which are much larger than the size of microbes, still remain.

Results of microbial filtration tests of the filter cloth are shown in Fig. 6. In contrast to the result that none of *E. coli* can be removed by two-layer cotton fabric, the filter cloth can clearly remove or immobilize the bacteria, and the removing percentage increases considerably as the number of layers increases. For example, about 30% of the *E. coli* can be removed by the two-layer filter cloth, while the six-layer filter cloth can remove almost all the bacteria.

As the pores and voids in the filter cloth are still much larger than the size of *E. coli*, and the introduction has mentioned that HA can adsorb bacteria efficiently, thus it is reasonable to believe that the removal of bacteria is mainly due to an adsorbing mechanism.

3.2. Porous ceramic

The XRD pattern of the sintered porous ceramic shows that it is composed of crystalline HA (Fig. 3b), which proves that there is no thermal decomposition of HA below the sintering temperature of 1200 °C.

SEM analysis of the structure of porous ceramics produced with WS reveals a microstructure composed of rather small pores that are suitable barriers for bacteria, as presented in Fig. 7, which shows that the WS can produce a large fraction of
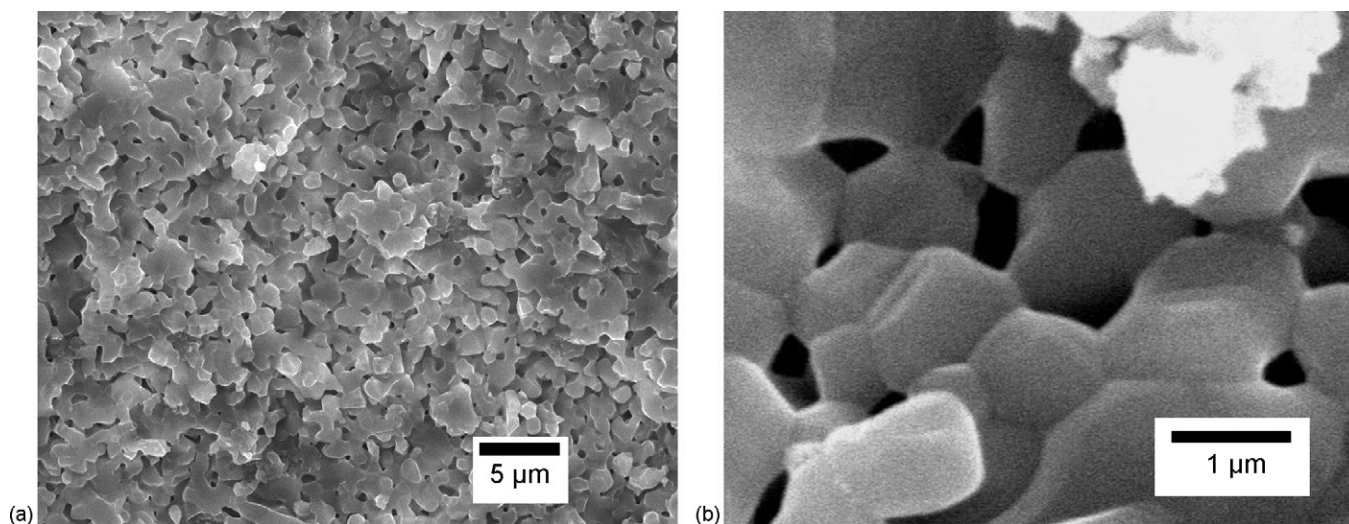

Fig. 7. SEM images showing (a) lots of small pores less than 3 μm produced with 30 vol% WS and (b) the submicron pores.
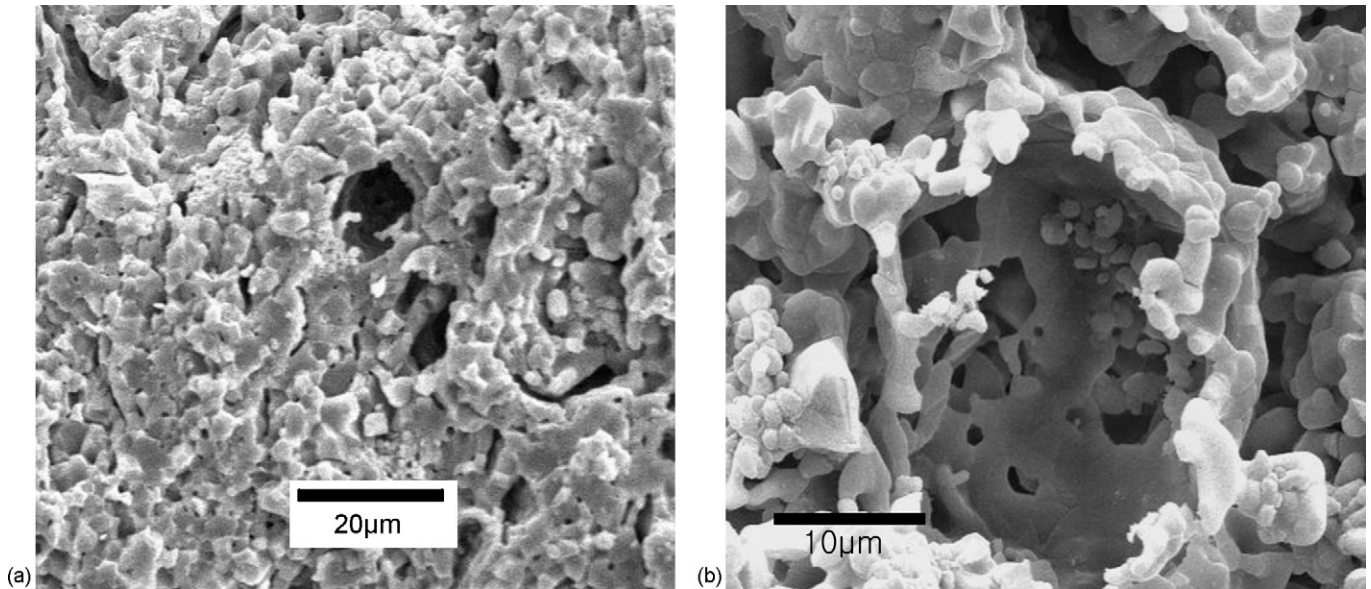
Fig. 8. SEM images showing (a) the presence of both large and small pores in the sample prepared with 15 vol% IS and 15 vol% WS and (b) details of a large pore, many small pores exist on the wall of a large pore.

small pores with diameters less than 3 μm, and most of them are submicron and isolated ones. The small pores always exist on grain boundaries and are surrounded by several grains nearby. These phenomena can be explained by the mechanism which has been discussed in our previous work [11]. It has demonstrated that the starch coating on the HA powders can produce more space among the particles and finally leave voids among the grains.

The porous ceramics produced by adding both WS and IS reveal the existence of both large and small pores, as shown in Fig. 8a. Our previous work shows that the large pores in the size of about tens micrometers are produced by adding IS as a pore former, and the small pores of several micrometers or less are mainly produced by using WS [11]. Fig. 8b shows the detail of a large pore and it can be seen that there are many small pores on its wall. Therefore, it can be inferred that, when both the WS and IS are added, many small pores can be interconnected and channeled by the large pores, and consequently, the specific surface area of the ceramic as well as the number of the sites to immobilize the microbes, are greatly increased.

The density and porosity data of the porous ceramics are listed in Table 2. The density decreases and the open porosity increases as the volume fraction of the starch increases. Obviously, the

volume fraction of IS has more influence on open porosity as it can form more large and interconnected pores. The data of open porosity also indicate that the small pores produced by WS are mainly isolated pores when the content of WS is not very high (<60 vol%). With the increase of WS, to 80 vol%, for example, the number of small pores increases and those isolated pores are more likely to connect together, which results in the predominance of open porosity in total porosity.

The relationship between the permeability of porous ceramics and the starch fraction shown in Fig. 9 is in agreement with the results of open porosity shown in Table 2. The permeability of the ceramics increases with increasing amounts of starch. The ceramics produced by only WS generally have low permeability, while the ones produced by using IS have much higher permeability. For example, the sample W2 produced by using as much as 60 vol% WS only have a permeability of 0.11×10^{-12} m^2, but the permeability of sample I produced by adding only 30 vol% IS reaches
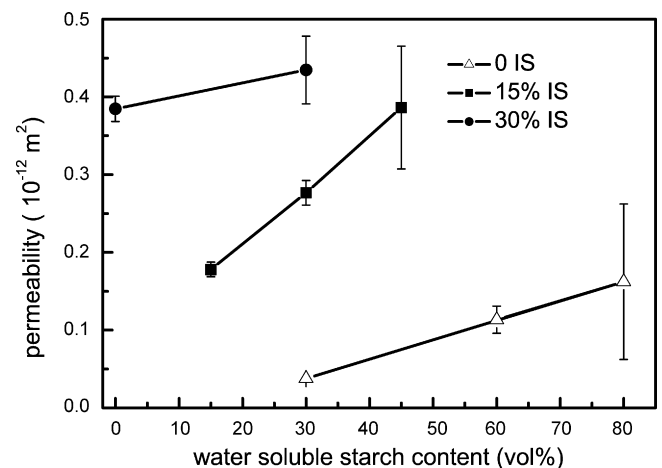
Table 2
Density and porosity data of porous ceramics

Sample	ρ_m (g/cm^3)	P_{tot} (%)	P_{open} (%)
I (30% IS)	2.16	31	21
W1 (30%WS)	2.63	15	6
W2 (60%WS)	2.01	36	20
W3 (80%WS)	1.30	58	31
M1 (15%IS + 15%WS)	2.43	22	14
M2 (15%IS + 30%WS)	2.17	35	23
M3 (15%IS + 45%WS)	1.83	41	28
M4 (30%IS + 30%WS)	1.55	50	38

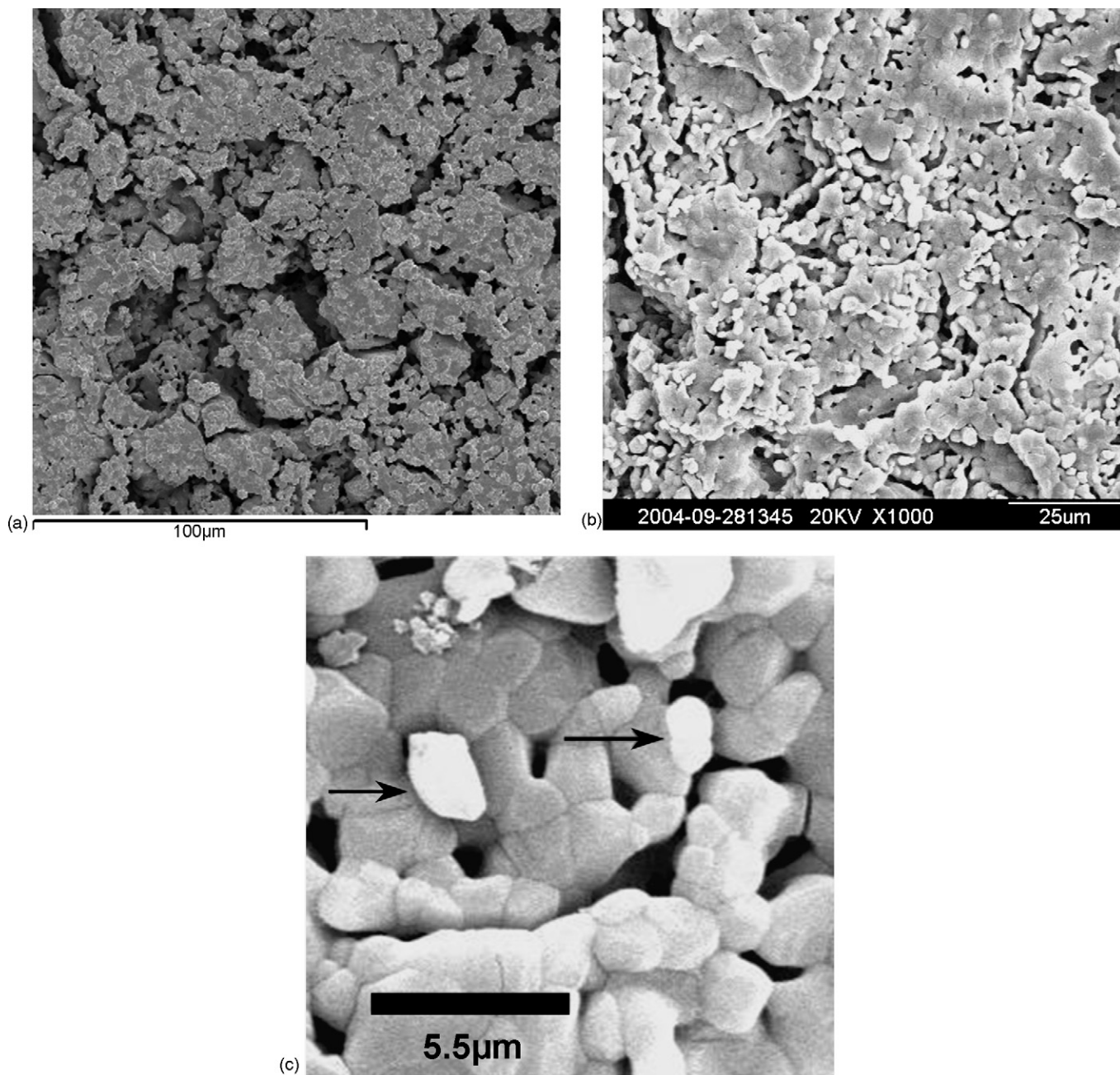Fig. 9. Permeability of the porous ceramics.

Fig. 10. SEM images showing the cross-section of the sample (a) before the microbial filtration; (b) after the microbial filtration and (c) magnification of the centre area of (b). In figures, the swell of the *E. coli* cells was due to vacuum.

0.38×10^{-12} m^2. As the volume fraction of WS increases, the permeability of samples prepared by using also IS (M1–M3) increases much faster than that of the ones prepared by using only WS (W1–W3), and the same trend occurs to the open porosity of these two series of samples. These phenomena can be attributed to the channeling of the small isolated pores by the large pores that are produced by adding IS, as shown in Fig. 8b.

According to Fig. 9, using different ratio and amounts of WS and IS can produce porous ceramic of almost any permeability below 0.4×10^{-12} m^2, and the proportion of large and small pores can also be controlled.

Sample M4 produced by using 30 vol% WS and 30 vol% IS was chosen to filter the *E. coli* suspension in the filtration test.

The samples were 2.40 mm in thickness and the SEM analysis showed the pore sizes of large and small pores were 10–30 μm and less than 3 μm, respectively. Results of the filtration test show that 100% of the *E. coli* can be removed by filtering through the porous ceramic. Comparing to other samples, M4 has much more large and interconnected pores as well as the highest porosity and permeability, therefore it is reasonable to assume that other samples also have such good microbial filtration properties.

Fig. 10 shows the cross sections of a sample before and after the microbial filtration test. We can see that many cells of *E. coli*, which are a bit larger than the true size of the *E. coli* because of the swelling in vacuum, are adsorbed on the porous

ceramic during the filtration test. Fig. 10c shows the magnification of the central area in Fig. 10b, the obstruction of *E. coli* cells by the small pores can also be observed. It is clear that the filtering mechanisms of the porous ceramic include both the absorption of microbes on HA and the barrier effect of the small pores.

4. Conclusions

HA powders smaller than 40 μm can be deposited tightly on fabric to produce stable filter cloth. This filter cloth can remove microbes in the fluid, and the filtration ability increases as the layers of the filter cloth increase. Six layers of the filter cloth are sufficient to remove all the *E. coli* cells in a suspension containing 10^5 cells/ml. The flexibility and coating stability of the filter cloth make it a good candidate for fabricating face masks and respirators.

The technique of using WS and IS is effective for preparing a dual porous structures of small pores less than 3 μm and large interconnected pores, respectively. A controllable permeability of the ceramic below 0.4×10^{-12} m^2, and a variable amount of small and large pores in ceramics can be obtained by varying the content and ratio of IS and WS.

The porous ceramic with a microstructure composed of both rather small pores and large pores has an excellent microbial filtration efficacy and good permeability. Besides the strong adsorption of microbes on HA, the small pores can enhance the filtration efficacy by acting as barriers. This kind of porous ceramic with controllable permeability and adjustable amount of small pores can fulfil either the requirement of complete microbial clearance like biomedical purification, or the fast filtration of contaminated fluids with low bacterial concentration.

References

[1] T. Driscoll, K. Steenland, D.I. Nelson, J. Leigh, Occupational airborne particulates: assessing the environmental burden of disease at national and local levels, Environmental burden of disease series no. 7, World Health Organization, 2004.
[2] L.L.J. Hench, Bioceramics: from concept to clinic, J. Am. Ceram. Soc. 74 (7) (1991) 1487–1491.
[3] H. Aoki, Medical Applications of Hydroxyapatite, Ishiyaku Euroamerica Inc., Tokio, 1994.
[4] M. Tomofumi, Japan Patent JP2002-053812A (19 February 2002).
[5] S. Tsuru, N. Shinomiya, Y. Katsura, Y. Uwabe, M. Noritake, M. Rokutanda, Adsorption and preparation of human viruses using hydroxyapatite column, Biomed. Mater. Eng. 1 (1991) 143–147.
[6] O. Lyckfeldt, J.M.F. Ferreira, Processing of porous ceramics by 'Starch Consolidation', J. Eur. Ceram. Soc. 18 (1998) 131–140.
[7] P. Sepulveda, F.S. Ortega, M.D.M. Innocentini, V.C. Pandolfelli, Properties of highly porous hydroxyapatite obtained by the gelcasting of foams, J. Am. Ceram. Soc. 83 (12) (2000) 3021–3024.
[8] Chinese Government Standard, Test method for apparent porosity and bulk density of porous ceramic, GB/T 1966–1996, 1996.
[9] D.R. Poirier, G.H. Geiger, Transport Phenomena in Materials Processing, The Mineral, Metals and Materials Society, Pennsylvania, 1994.
[10] ISO 8841:1991. Dense shaped refractory products-Determination of permeability to gases, 1991.
[11] L. Yang, X.S. Ning, K.X. Chen, Q.F. Xiao, H.P. Zhou, Preparation of porous hydroxyapatite ceramics with starch additives, Trans. Nonferrous Met. Soc. China 15 (2) (2005) 257–260.